HHS Public Access

Author manuscript

Cell Rep. Author manuscript; available in PMC 2019 June 03.

Published in final edited form as:

Cell Rep. 2019 April 09; 27(2): 374–386.e4. doi:10.1016/j.celrep.2019.03.035.

Transient Kinetic Analysis of SWR1C-Catalyzed H2A.Z Deposition Unravels the Impact of Nucleosome Dynamics and the Asymmetry of Histone Exchange

Raushan K. Singh[1,3], **Jiayl Fan**[1,3], **Nathan Gioacchini**[1], **Shinya Watanabe**[1], **Osman Bilsel**[2], and **Craig L. Peterson**[1,4,*]

[1]Program in Molecular Medicine, University of Massachusetts Medical School, Worcester, MA 01605, USA

[2]Department of Biochemistry and Molecular Pharmacology, University of Massachusetts Medical School, Worcester, MA 01655, USA

[3]These authors contributed equally

[4]Lead Contact

SUMMARY

The SWR1C chromatin remodeling enzyme catalyzes ATP-dependent replacement of nucleosomal H2A with the H2A.Z variant, regulating key DNA-mediated processes such as transcription and DNA repair. Here, we investigate the transient kinetic mechanism of the histone exchange reaction, employing ensemble FRET, fluorescence correlation spectroscopy (FCS), and the steady-state kinetics of ATP hydrolysis. Our studies indicate that SWR1C modulates nucleosome dynamics on both the millisecond and microsecond timescales, poising the nucleosome for the dimer exchange reaction. The transient kinetic analysis of the remodeling reaction performed under single turnover conditions unraveled a striking asymmetry in the ATP-dependent replacement of nucleosomal dimers, promoted by localized DNA unwrapping. Taken together, our transient kinetic studies identify intermediates and provide crucial insights into the SWR1C-catalyzed dimer exchange reaction and shed light on how the mechanics of H2A.Z deposition might contribute to transcriptional regulation *in vivo*.

In Brief

The SWR1C remodeling enzyme catalyzes ATP-dependent replacement of nucleosomal H2A with the H2A.Z variant at promoter-proximal nucleosomes. Singh et al. investigate the transient kinetic

*Correspondence: craig.peterson@umassmed.edu.

AUTHOR CONTRIBUTIONS

Experiments were performed by R.K.S. and J.F. N.G. helped with SWR1C purification and nucleosome reconstitution. S.W. helped with histone purification. O.B. assisted with the FCS studies. C.L.P., R.K.S., and J.F. analyzed the data and prepared the manuscript.

DECLARATION OF INTERESTS

The authors declare no competing interests.

SUPPLEMENTAL INFORMATION

Supplemental Information can be found online at https://doi.org/10.1016/j.celrep.2019.03.035.

mechanism of this histone exchange reaction and show that SWR1C transiently unwraps nucleosomal DNA, promoting a concerted dimer eviction and replacement reaction.

Graphical Abstract

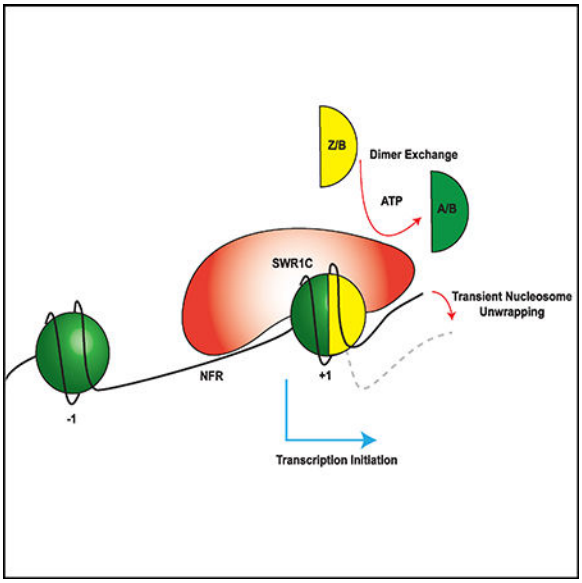

INTRODUCTION

Eukaryotic genomes are assembled into long, linear arrays of nucleosomes that each consist of an octamer of core histones around which ~147 bp of DNA is wrapped nearly two times. The histone octamer is composed of a central hetero-tetramer of histones H3 and H4 flanked by two heterodimers of histones H2A and H2B. Within the nucleosome, the H3/H4 tetramer wraps the central ~90 bp of nucleosomal DNA, whereas each H2A-H2B dimer organizes and stabilizes the final few turns (Luger et al., 1997). *In vivo*, nucleosomal arrays are highly heterogeneous. Nucleosomes are precisely positioned around regulatory regions such as gene promoters or replication origins, different genomic regions harbor histones with a variety of posttranslational modifications, and the canonical core histones can be replaced with a number of conserved histone variants (Yuan et al., 2005; Raisner et al., 2005; Jiang and Pugh, 2009; Venkatesh and Workman, 2015). These complex chromatin structures are often highly dynamic and can provide epigenetic information that regulates gene expression, replication timing, and other key nuclear processes (Swygert and Peterson, 2014; Henikoff, 2016)

Transcription in a eukaryotic cell can be regulated by the structure and dynamics of nucleosomes located immediately upstream and downstream of the transcription start site (TSS) (Cairns, 2009; Dion et al., 2007). These promoter-proximal nucleosomes flank a nucleosome-depleted region (NDR) of ~200 bp and are highly enriched for the conserved histone variant H2A.Z (Hartley and Madhani, 2009; Barski et al., 2007). The H2A.Z variant is an evolutionarily conserved variant of H2A whose incorporation into a nucleosome modulates its dynamics and promotes intramolecular folding of nucleosomal arrays (Fan et

al., 2002; Park et al., 2004). In budding yeast, H2A.Z is enriched in the promoter regions of both active and inactive genes, and H2A.Z is known to play a key role in promoting the proper kinetics of transcriptional activation (Santisteban et al., 2000; Raisner et al., 2005). In addition, yeast H2A.Z is enriched within nucleosomes that flank replication origins as well as at the boundaries of heterochromatic regions, where it mediates an anti-silencing effect by preventing the ectopic spread of heterochromatin (Albert et al., 2007; Meneghini et al., 2003). Likewise, in higher metazoans, H2A.Z is enriched at pericentric heterochromatic regions during the early stages of embryonic development (Banaszynski et al., 2010). In addition to its critical role in transcription, H2A.Z has been intimately linked with DNA repair pathways and the regulation of cell cycle checkpoints, hallmarks of genome integrity (Adkins et al., 2013; Xu et al., 2012; Gévry et al., 2007). Not surprisingly, yeast cells lacking H2A.Z show temperature-sensitive growth defects and are sensitive to various genotoxic agents (Santisteban et al., 2000). Moreover, loss of H2A.Z in the frog and mouse causes embryonic lethality (Faast et al., 2001).

Unlike canonical histones, which are primarily assembled by a replication-dependent mechanism, H2A.Z is deposited at precise nucleosomal positions in an ATP-dependent reaction by enzymes related to the yeast SWR1C chromatin remodeling enzyme (Kobor et al., 2004; Mizuguchi et al., 2004). There are four subfamilies of chromatin remodeling enzymes—SWI-SNF, CHD, ISWI, and INO80—that are evolutionarily conserved from yeast to humans (Clapier et al., 2017). Many chromatin remodelers are enormous multi-subunit enzymes that each contain a related catalytic subunit that harbors a bi-lobular, RecA-like ATPase domain. SWR1C and its mammalian paralogs SRCAP and p400/Tip60 are members of the INO80C subfamily, and they use the energy of ATP hydrolysis to catalyze a histone exchange event where each of the two nucleosomal H2A-H2B dimers is sequentially replaced with H2A.Z-H2B variant dimers (Ruhl et al., 2006; Luk et al., 2010). Unlike all other chromatin remodelers that can use their ATP-dependent, DNA translocase activity to "slide" nucleosomes along DNA *in cis*, SWR1C can deposit H2A.Z without altering nucleosome positions (Clapier et al., 2017; Bowman 2010; Ranjan et al., 2015). To specifically direct the deposition of H2A.Z at promoter-proximal nucleosomes, SWR1C is targeted to promoter regions by interactions with free DNA at the NDR, targeting the adjacent +1 and 1 nucleosomes (nucleosomes are numbered relative to the TSS) (Ranjan et al., 2013). Likewise, the mammalian SRCAP and p400/Tip60 enzymes are believed to be targeted to promoter regions by gene-specific regulators (Pradhan et al., 2016; Yildirim et al., 2011).

The biological function of proteins requires local and global conformational fluctuations that take place in the micro- to millisecond timescale (Henzler-Wildman and Kern, 2007). Nucleosomes can undergo spontaneous conformational fluctuations on the millisecond timescale that facilitate the transient accessibility of nucleosomal DNA to nuclear factors (Li and Widom 2004; Li et al., 2005). However, it remains unclear how remodeling enzymes such as SWR1C modulate the conformational dynamics of the nucleosome during an ATP-dependent nucleosome remodeling reaction. Notably, the SWR1C-catalyzed dimer exchange reaction is complex, requiring fine-coupling of the energy of ATP hydrolysis to several microscopic events of the nucleosome remodeling reaction (Zhou et al., 2016). Therefore, this nucleosome remodeling cycle is expected to contain multiple intermediates that may

remain invisible in discontinuous and/or steady-state biochemical assays. Transient kinetic experiments are well suited to unravel the identity of reaction intermediates and microscopic rate constants associated with their production and decay and, hence, provide in-depth mechanistic analysis of an enzyme-catalyzed reaction (Jencks 1989; Fersht 1999).

Here we investigate the transient kinetic mechanism of the SWR1C-catalyzed dimer exchange reaction employing ensemble fluorescence resonance energy transfer (FRET), fluorescence correlation spectroscopy (FCS), and steady-state kinetics of ATP hydrolysis. We find that SWR1C utilizes an ATP-dependent modulation in nucleosome dynamics on the microsecond timescale as a strategy for discriminating the two structurally similar H2A and H2A.Z nucleosomes. In addition, our FRET studies indicate that free H2A.Z-H2B dimers function as essential co-substrates that stimulate SWR1C ATPase activity and promote unwrapping of DNA at the nucleosomal edge. This ATP-dependent unwrapping of nucleosomal DNA occurs on the same timescale as H2A-H2B eviction and replacement, suggesting that it is an obligatory step in the reaction. Finally, our transient kinetic studies uncover asymmetry in the H2A.Z deposition reaction, where a linker-distal dimer is replaced first, followed by the slower replacement of the linker-proximal dimer. The asymmetry of the H2A.Z deposition reaction suggests a regulatory role for gene transcription and provides insights into the molecular mechanism of ATP-dependent nucleosome remodeling catalyzed by other families of chromatin-remodeling enzymes.

RESULTS

Dynamic Nucleosome Fluctuations Specify a Substrate Competent for SWR1C Remodeling

To investigate the transient kinetic mechanism of the SWR1C-catalyzed histone dimer exchange, a fluorescence-based strategy was employed. End-positioned, recombinant yeast mononucleosomes were assembled on an ~200-bp fragment containing a “601” nucleosome positioning sequence (Figure 1A). The nucleosomal substrates were designed with 55–77 bp of flanking linker DNA so that it might reflect the asymmetry of a promoter-proximal nucleosome located next to a NDR. In most cases, mononucleosome substrates contain a Cy3 fluorophore covalently attached to the linker-distal end of the nucleosomal DNA, and Cy5 was attached to either the H2A C-terminal domain or the H3 N-terminal domain. The Cy3 and Cy5 fluorophores are within an appropriate distance to function as a FRET pair so that excitation of the Cy3 donor with a 530-nm light source leads to efficient energy transfer to the Cy5 acceptor, as evidenced by the fluorescence emission peak at 670 nm (Li and Widom, 2004; Figure S1).

Previous studies have demonstrated that nucleosomes undergo spontaneous unwrapping and/or rewrapping of nucleosomal DNA on the millisecond timescale (Li and Widom 2004; Li et al., 2005). To investigate the effect of SWR1C on this dynamic behavior, we investigated nucleosome dynamics utilizing FRET-FCS and a nucleosomal substrate that contains Cy3 on the linker-distal nucleosomal edge and Cy5 on the H2A C terminus (55N0; Figures 1A and 1B; Torres and Levitus, 2007). In this assay, the conformational fluctuations of the nucleosome are determined from the ratio of the auto-correlation and cross-correlation functions of the change in fluorescence intensity of the acceptor (Cy5) and donor-acceptor (Cy3-Cy5) pair (Figures 1C and 1D). Utilizing FRET-FCS, the observed rate constant (k_{obs})

for nucleosomal DNA unwrapping and/or rewrapping was determined to be ~7 s^{-1} (half-life = ~100 ms) (Figure 2A), slightly slower than values reported previously for a vertebrate nucleosome (~21 s^{-1}) (Li et al., 2005). Likewise, the dynamics of an H2A.Z nucleosome were similar, with a k_{ob} of ~2.1 s^{-1} (half-life = 330 ms) (Figure 2D). Strikingly, binding of SWR1C to either an H2A or H2A.Z nucleosome increased the rate of DNA unwrapping and/or rewrapping by ~2 orders of magnitude compared with the unbound nucleosome (half-life = 1 ms) (Figures 2B and 2E; Figure S2; Table S1). Furthermore, addition of AMP-PNP further altered the dynamics of the SWR1C-H2A nucleosome complex, yielding a markedly biphasic pattern (Figure 2C). The two phases had nearly equal amplitudes, and the k_{obs} for the fast and slow phases were 40 s^{-1} (half-life = ~1 ms) and ~5×10^4 s^{-1} (half-life = ~14 μs), respectively (Figure 2C; Figure S1; Table S1). We note that there may also be a fast component when SWR1C is bound to the H2A nucleosome in the absence of nucleotides, although, in this case, the amplitude is small and may not be significant (Table S1). Likewise, addition of AMP-PNP had no significant effect on the dynamics of an SWR1C-H2AZ nucleosome complex (Figure 2F), suggesting that the enhanced microsecond dynamics are linked to substrate discrimination and that they may help SWR1C to select the appropriate nucleosomal conformation that can be funneled to the next step of the dimer exchange reaction.

H2A.Z-H2B Dimers Activate Dimer Eviction by SWR1C

One consequence of enhanced nucleosomal DNA wrapping/unwrapping might be the eviction or destabilization of H2AH2B dimers prior to their replacement with H2A.Z-H2B. To monitor eviction of H2A-H2B dimers, an H2A nucleosome was reconstituted that contained unlabeled nucleosomal DNA and a Cy3-Cy5 FRET pair located on the histone H3 N terminus and the H2A C terminus, respectively (Figure S3A). To directly probe for changes in histone-histone interactions in real-time, we monitored changes in the nucleosomal FRET acceptor (Cy5) signal catalyzed by SWR1C under single-turnover conditions (excess enzyme to substrate). Notably, no changes in the FRET signal were observed during incubation with SWR1 and ATP, indicating that enhanced DNA unwrapping/wrapping dynamics are not sufficient for dimer eviction (Figure S3A).

Previous studies have demonstrated that H2A.Z-H2B dimers function as co-substrates in the SWR1C exchange reaction, stimulating ATPase activity and interacting with both the Swr1 ATPase and the Swc2 subunit (Luk et al., 2010; Hong et al., 2014, Wu et al., 2005). Strikingly, addition of free H2A.Z-H2B dimers to the SWR1C remodeling reaction (H3-Cy3/H2A-Cy5 FRET substrate) led to a robust, extensive loss of Cy5 signal from the nucleosomal FRET substrate in an ATP-dependent reaction, indicating that H2A.Z-H2B dimers are essential co-factors for H2A-H2B eviction (Figure S3A). Eviction of H2A-H2B dimers was also monitored with the nucleosomal FRET substrate containing a Cy3-labeled DNA terminus and Cy5-labeled histone H2A (55N0; Figure 3A). In this case as well, addition of both SWR1C and free H2A.Z-H2B dimers led to a dramatic, ATP-dependent decrease in the FRET signal, consistent with eviction of the Cy5-labeled H2A-H2B dimers (Figure 3B). Importantly, the ATP- and H2A.Z-H2B-dependent loss of the Cy5 signal was accompanied by a reciprocal increase in the Cy3 signal, consistent with a loss of FRET (Figure S3B). Notably, addition of free H2A-H2B dimers did not alter the Cy5 FRET signal,

nor did H2A.Z-H2B dimers promote dimer loss from an H2A.Z nucleosome, results fully consistent with proper substrate specificity (Figure S3C). In addition, the H2A.Z-H2B-dependent loss of FRET was not observed on a substrate that contained a pair of 2-nt DNA gaps at nucleosomal superhelical location (SHL) ±2.0, indicating that an intact SHL2 is essential for dimer eviction, as predicted by an earlier study (Figure 3C; Ranjan et al., 2015).

SWR1C Induces Unwrapping of DNA at the Nucleosomal Edge

A wealth of data support the unifying view that chromatin remodeling enzymes perform their various functions by initiating an ATP-dependent DNA translocation event from a fixed point on the nucleosome surface, in most cases about two DNA helical turns from the nucleosomal dyad (SHL ±2.0) (Clapier et al., 2017). Indeed, SWR1C has been shown to make tight contact with nucleosomal DNA at SHL2.0, and single-strand DNA gaps near SHL2.0 block H2A.Z deposition *in vitro*, suggesting an essential role for DNA translocation by SWR1C (Ranjan et al., 2015). However, unlike other remodeling enzymes, prior assays have not observed stable alterations in nucleosome positioning because of the SWR1C remodeling reaction (Luk et al., 2010; Ranjan et al., 2015). One possibility is that SWR1C promotes only a limited amount of DNA translocation that could provide the initial trigger for dimer eviction.

In an initial attempt to directly probe for changes in DNA-histone interactions, the steady-state conformation of a 77N0 nucleosome (H2A-Cy5) was monitored by a wavelength scan of SWR1C reactions containing SWR1C alone, SWR1C and AMP-PNP, or SWR1C and ATP (Figure 4A). Interestingly, addition of saturating amounts of SWR1C led to an increase in the Cy3 signal and an increase in the Cy5 FRET signal (likely because of the increase in Cy3), indicating that binding of SWR1C alters the solvent micro-environment of the nucleosomal edge. Interestingly, further incubation with either AMP-PNP or ATP did not lead to a significant change in either Cy3 or Cy5 emissions, indicating that binding and hydrolysis of ATP does not lead to stable changes in nucleosome structure that could be detected with this FRET pair.

To further investigate the potential for DNA translocation, FRET time courses were performed under single-turnover conditions (excess SWR1C to nucleosome) to probe for transient changes in histone-DNA interactions. A nucleosomal substrate was assembled that harbored the Cy5 fluorophore on the H3 N-terminal domain and Cy3 on a short, 3-bp distal linker (Figure 1A). The potential advantage of this substrate is that changes in DNA-histone interactions can be monitored even when the resident H2A-H2B dimer is replaced, unlike the case where Cy5 labels H2A. Furthermore, we anticipated that movement of DNA from the short linker toward the nucleosome edge might give rise to an ATP-dependent change in FRET. However, addition of ATP and SWR1C did not significantly alter the FRET signal (Figure 4B). Surprisingly, further addition of free H2A.Z-H2B dimers also did not change the FRET signal, even though the distal H2A-H2B dimer would be evicted during this time course (Figure 4B).

Under standard reaction conditions, the dimer eviction reaction has a half-life of ~2 min (Figure 3B), which may preclude detection of transient, small changes in FRET. To slow the rate of dimer exchange, the ATP concentration was reduced 100-fold so that the

concentration was ~10-fold below K_M (Luk et al., 2010). At this lower ATP concentration, the initial rate of dimer eviction showed a half-life of ~6 min using the 77N0 substrate (H2A-Cy5) (Figure S4A). Surprisingly, even under these conditions, no significant changes in FRET could be detected when SWR1C and ATP were added to the H3-Cy5 substrate that reports on changes in DNA-histone interactions (77N3 substrate; Figures 1A and 4C). Strikingly, however, further addition of free H2A.Z-H2B dimers led to a transient decrease in FRET, followed by an increase (Figure 4C). Importantly, small changes in Cy5 emission observed after direct Cy5 excitation were not ATP-dependent, eliminating the possibility that changes were due to an altered solvent environment during the dimer exchange reaction (Figure 4D). In addition, this transient decrease in FRET was not observed for reactions containing AMP-PNP and H2A.Z-H2B dimers, demonstrating a requirement for ATP hydrolysis (Figure 4C). Importantly, the rate of FRET decrease was faster than the rate of dimer eviction under these low-ATP conditions ($t_{1/2}$ = 2.1 min), consistent with an ATP-dependent, on-pathway reaction (Figure 4C; Figure S4B). These results suggest that SWR1C promotes ATP-dependent unwrapping of DNA at the nucleosomal edge only in the presence of free H2A.Z-H2B dimers.

The SWR1C-Catalyzed Replacement of H2A-H2B Dimers Is Markedly Asymmetric

The kinetic trace of the dimer eviction reaction revealed a markedly biphasic reaction (Figure 3B). The experimental data were analyzed with a double-exponential rate equation, yielding values for the fast and slow k_{obs} of 0.33 min^{-1} (half-life = 2.1 min) and 0.06 min^{-1} (half-life = 12.3 min), respectively. In addition, the fast phase of the reaction was associated with an ~70% change of the FRET amplitude, whereas there was a smaller, ~30% amplitude associated with the slow phase. One possibility is that the two distinct kinetic phases reflect the sequential SWR1C-catalyzed eviction and replacement of each of the two H2A-H2B dimers under these single-turnover conditions. To further investigate this possibility, we measured the kinetics for ATP-dependent deposition of H2A.Z-H2B. For monitoring H2A.Z deposition, the nucleosomal substrate contained a Cy3 fluorophore on the nucleosomal DNA edge, and the free H2A.Z-H2B dimer contained the Cy5 label on the H2A.Z C terminus (Figure 5A). SWR1C reactions were initiated under single-turnover conditions, and the kinetic trace shows an ATP-dependent increase in the FRET signal, consistent with H2A.Z deposition (Figure 5B). Importantly, the kinetic profile for H2A.Z deposition was also clearly biphasic, yielding k_{obs} for the fast and slow phases of 0.32 min^{-1} (half-life = 2.2 min.) and 0.04 min^{-1} (half-life = 16.6 min), respectively. Notably, the values of these k_{obs} for H2A.Z-H2B deposition are quantitatively similar to those of the fast and slow k_{obs} measured for the eviction of H2A-H2B (Figure 3B). Taken together, the remarkable similarity in the biphasic kinetic profiles suggests that SWR1C catalyzes sequential exchange of two H2A-H2B dimers in a real-time assay performed under single-turnover conditions.

The biphasic kinetics of dimer eviction and deposition may reflect asymmetry in the catalytic cycle so that the first round of dimer exchange occurs preferentially on one face of the nucleosome with a rate that is ~6-fold faster than exchange of the second dimer. To address this question, FRET mononucleosomes were reconstituted that contained single, 2-nt gaps in nucleosomal DNA at either the linker-proximal (SHL−2.0) or linker-distal (SHL

+2.0) regions (Figures 3D, 3E, 5D, and 5E). These substrates were used in dimer eviction or dimer deposition reactions performed under single-turnover conditions with SWR1C, H2A.Z-H2B dimers, and ATP. Notably, the ATP-dependent kinetic profiles for these gapped substrates were monophasic, in sharp contrast to the mononucleosomes with intact nucleosomal DNA. For instance, when the 2-nt gap was located at linker-distal SHL+2.0, only a slow phase (k_{obs} = 0.06 min^{-1}) of FRET loss was observed in the dimer eviction assay, and the change in FRET amplitude was small (Figure 3D). Likewise, only a slow phase of H2A.Z deposition was observed in the FRET deposition assay (Figure 5D). In contrast, when the gap was located at the linker-proximal SHL−2.0, only a fast phase (k_{obs} = 0.12 min^{-1}) of FRET loss or deposition remained (Figure 3E and 5E). Furthermore, this fast phase was associated with a much larger drop or gain in FRET amplitude (~70%) compared with the slow phase, indicating that the fast phase reflects removal and replacement of the dimer closest to the distal, Cy3-labeled DNA. Together, these results indicate that SWR1C preferentially evicts and replaces the H2A-H2B dimer located at the linker-distal half of the nucleosome, followed by a slower reaction where the linker-proximal H2A-H2B dimer is replaced.

The 601 nucleosome positioning sequence is inherently asymmetric, containing a set of periodic TpA (TA) dinucleotide steps that is more prevalent on one side of the dyad compared with the opposite side. This asymmetry is known to affect the unwrapping properties of nucleosomal DNA as well as to regulate the efficiency of nucleosome repositioning by the Chd1 remodeling enzyme (Ngo et al., 2015; Winger and Bowman, 2017). One possibility is that the asymmetry of the 601 sequence is responsible for the biphasic kinetics of dimer exchange. In our substrates, the TA-rich side of the 601 sequence, which stabilizes DNA wrapped on the nucleosome, is positioned on the linker-distal side of the nucleosome, where the first, rapid round of dimer exchange occurs (77N0 substrate). We assembled a “flipped” 0N77 FRET substrate that places the TA-rich side of the 601 adjacent to the long linker. The rates of dimer exchange were tested in parallel for both the 770N and 077N FRET substrates, which harbor H2A-Cy5 and DNA labeled with Cy3 at the distal DNA end. As shown in Figure 6A, the dimer exchange reaction remained biphasic with both substrates, and the rate of the first, rapid phase of the reaction was identical between substrates. However, the second round of dimer exchange was slower with the 0N77 substrate. These results indicate that the asymmetry in the 601 sequence does not affect the overall asymmetry of the SWR1C-catalyzed dimer exchange reaction, but the DNA sequence does have a significant effect on the rate of the second round of dimer exchange.

Biphasic kinetics indicate that the two rounds of dimer exchange occur at different rates. One possibility is that the first round of exchange is faster because linker DNA not only orients the enzyme to initially attack the linker-distal dimer but that it also stimulates the reaction. Alternatively, the second round of dimer exchange may simply be an inherently slower reaction. To test these possibilities, we reconstituted a centrally positioned, 257-bp nucleosome that harbors a Cy3/Cy5 FRET pair on the histone H3 N-terminal and H2A C-terminal domains, respectively (Figure 6B). If asymmetric linker DNA is responsible for biphasic kinetics, then the centrally positioned nucleosome should show a monophasic profile, whereas biphasic kinetics should still be observed if the second round is inherently slow. Strikingly, the centrally positioned nucleosome showed clear biphasic kinetics of

dimer eviction, with rates similar to those observed for the end-positioned substrate (Figure 5B; $t_{1/2\ fast}$ = 0.6 min, $t_{1/2\ slow}$ = 9.4 min). Thus, having a long linker DNA on one end of a positioned nucleosome, as observed for the +1 nucleosome at promoter regions, functions primarily to orient the enzyme so that the linker-distal dimer is displaced first. The second round of dimer exchange appears to be an inherently slower reaction, perhaps because the H2A.Z/H2A heterotypic intermediate is a poor substrate.

SWR1C-Nucleosome Interactions Couple ATPase Activity to Dimer Eviction

Remodeling enzymes couple the energy of ATP hydrolysis to translocation of DNA, and, in many cases, gaps at SHL2.0 block remodeling activities (Figure 3 and 5; Ranjan et al., 2015). Previous studies have shown that the basal ATPase activity of SWR1C is stimulated by both the nucleosomal substrate and the H2A.Z-H2B co-substrate (Figure S5A; Luk et al., 2010). To probe the effect of intact nucleosomal DNA on the chemo-mechanical coupling of SWR1C ATPase activity, steady-state ATPase assays were performed with a nucleosomal substrate that contains 2-nt gaps at both SHL+2.0 and SHL2.0 (Figures S5B and S5C). Strikingly, the gapped nucleosome was unable to stimulate the ATPase activity of SWR1C (Figure S5B). Thus, the stimulation of SWR1C ATPase activity by nucleosomes reflects efficient coupling of ATP hydrolysis to productive interactions with DNA. In sharp contrast, gaps in nucleosomal DNA did not diminish the effect of H2AZ-H2B but led to a further, ~1.5× increase in the steady-state rate (Figure S5B). Thus, on a gapped nucleosome, the H2AZ-H2B dimers stimulate the rate of hydrolysis, reflecting apparent uncoupling of ATP hydrolysis from its effects on nucleosomal DNA. The effect of the gap appears to be similar to the ATPase cycle of AAA+ chaperones, which undergo rapid hydrolysis of ATP upon encountering a very stable substrate that is resistant to ATP-dependent unfolding (Sauer and Baker, 2011).

DISCUSSION

SWR1C is unique among remodeling enzymes because it cannot mobilize nucleosomes *in cis*, but, rather, it is dedicated to the ATP-dependent replacement of nucleosomal H2A with its variant, H2A.Z (Clapier et al., 2017). In contrast to previous studies of ATP-dependent nucleosome sliding reactions, we found that the dimer exchange reaction is kinetically slow, likely because the reaction has to transit multiple activation or transition state barriers during the catalytic cycle (Hammes, 2002). Furthermore, the coordination of several different microscopic events associated with each round of dimer exchange—DNA unwrapping, H2A-H2B eviction, and H2A.Z-H2B deposition—is likely to yield a large number of kinetic intermediates. Here we probed for such steps using several biophysical approaches, including the use of single-turnover reaction conditions in which excess enzyme synchronizes the system at the beginning of the reaction cycle and it remains synchronous until the substrate completes one reaction cycle.

Our transient kinetic investigation supports a complex reaction pathway involving at least five distinct intermediates (Figure 7). In step 1, binding of SWR1C to an end-positioned, asymmetric nucleosome yields a SWR1C-nucleosome complex that has an ~100-fold enhanced rate of DNA wrapping/unwrapping. Nucleosome recognition also appears to

anchor the Swr1 ATPase to nucleosomal DNA, enhancing the affinity for ATP and coupling subsequent ATP hydrolysis to DNA manipulations. In step 2, binding of ATP leads to additional enhancement of nucleosome dynamics on the microsecond timescale that are unique to an H2A nucleosomal substrate. In step 3, free H2A.Z-H2B dimers act as a power stroke, promoting ATP hydrolysis and unwrapping of DNA at the nucleosomal edge. In step 4, the preceding power stroke drives the initial eviction of the linker-distal H2A-H2B dimer and replacement by H2A.Z-H2B in an apparently concerted reaction. In step 5, the second, linkerproximal dimer is sequentially replaced during the single-turnover reaction cycle with kinetics at least 6-fold slower than the first replacement event. These slower kinetics may be due to an inherent difficulty in remodeling the H2A/H2A.Z heterotypic intermediate, a possibility that can be tested in the future by assembly of oriented hexosomes, as described by Qiu et al. (2017). Below, we discuss in greater detail the mechanistic implications for this reaction series.

Conformational Fluctuations of the Nucleosome during the Dimer Exchange Reaction

Macromolecules undergo spontaneous conformational fluctuations, leading to ensembles of multiple, distinct conformations (Henzler-Wildman and Kern, 2007). Notably, biophysical studies have shown that such “wiggling and giggling” in proteins or enzymes is indispensable for their function and that these dynamics often affect enzyme-substrate specificity and are kinetically coupled with their catalytic turnover rate (Feynman and Sands, 1963; Agarwal et al., 2002; Henzler-Wildman et al., 2007). The nucleosome is known to undergo spontaneous conformational fluctuations on the millisecond timescale, manifested in the unwrapping and rewrapping of nucleosomal DNA (Li and Widom 2004; Tims et al., 2011). Additional conformational fluctuations are also likely to involve the entire nucleosome (Henzler-Wildman and Kern, 2007), including the histone octamer, and such dynamics are expected to influence remodeling reactions.

We found that the binding of SWR1C to a canonical H2A nucleosome is characterized by an ~100-fold increase in the rate of nucleosome conformational fluctuations on the millisecond timescale. Faster unwrapping and/or rewrapping kinetics of the nucleosomal DNA end are likely to facilitate the eviction of H2A-H2B dimers because the dimers are tightly held within the nucleosome via a strong electrostatic interaction with the last 3 superhelical turns (SHL±3.5–6.5) of nucleosomal DNA (Luger et al., 1997). Additionally, these conformational fluctuations may also promote the generation of early intermediates of the dimer exchange reaction by reducing the activation energy barrier for approaching the transition state (Daniel et al., 2003; Nashine et al., 2010). This viewpoint is strengthened by our observation that ATP binding induces additional nucleosomal fluctuations on the microsecond timescale, changes that are not observed when SWR1C is bound to the remodeling product, the H2A.Z nucleosome. Such a stark difference in the conformational fluctuations between an H2A and H2A.Z nucleosome underscores the idea that kinetic coupling of nucleosomal conformational fluctuations may be critical for progression of the ATP-dependent dimer exchange reaction cycle (Eisenmesser et al., 2002). Notably, a similar effect of ATP binding on SWR1C-induced nucleosome fluctuations has recently been

described in a single-molecule FRET approach (Willhoft et al., 2018). We also envision that ATP-dependent nucleosome dynamics may facilitate the ability of SWR1C to search for an appropriate conformation of nucleosomes to be funneled into the catalytic cycle (Vendruscolo and Dobson 2006). Notably, the catalytic efficiency of an enzyme is often linked with the kinetics of a conformational search of both the enzyme and its cognate substrate (Benkovic and Hammes-Schiffer 2003). Thus, in this view, the ATP-bound SWR1C-H2A.Z-nucleosome complex may be kinetically trapped at the beginning of the catalytic cycle.

Nucleosome Recognition by INO80C and SWR1C

Recently, studies have reported cryoelectron microscopy (cryo-EM) reconstructions of the yeast and human INO80C remodeling enzymes bound to an end-positioned nucleosome (Eustermann et al., 2018; Ayala et al., 2018), as well as a cryo-EM structure of nucleosome-bound SWR1C (Willhoft et al., 2018). INO80C is highly related to SWR1C, having a similar subunit module organization and sharing several subunits, such as the Rvb1/Rvb2 heterohexomeric ring assembly (Watanabe et al., 2015). Remarkably, INO80C and SWR1C use similar but distinct strategies to engage an end-positioned nucleosome (one side contains a long DNA linker). First, both enzymes bind the nucleosome within a large cleft between two lobes; one lobe contains the ATPase domain, and the second lobe contains a group of key subunits. In the case of INO80C, the two lobes interact along nearly an entire gyre of nucleosomal DNA on the linker-proximal side of the nucleosome, with the ATPase lobes of the Ino80 subunit making tight contact with DNA at the linker-proximal SHL-6 region and the Ies2/Ies6/Arp5 subunit module interacting with DNA at SHL-2 (Eustermann et al., 2018). These interactions position INO80C to initiate DNA translocation from the nucleosomal edge proximal to the long linker, pulling the linker DNA into the nucleosome, toward the subunit module bound at SHL-2.0, eventually leading to re-positioning of the nucleosome toward the center of the DNA fragment.

Strikingly, SWR1C has a similar interaction with the nucleosome, but, in this case, the two large lobes interact with the opposite gyre of nucleosomal DNA, and their orientation is switched; the Swr1 ATPase lobes interact with SHL+2.0, and the Swc2/Arp6/Swc6/Swc3 module interacts with SHL+6.0 (Willhoft et al., 2018). This orientation positions SWR1C so that translocation occurs from the more canonical SHL2 position, pulling DNA toward the nucleosomal dyad from the linker-distal DNA end. These interactions are fully consistent with prior hydroxyl radical footprinting studies for both INO80C and SWR1C (Brahma et al., 2017; Ranjan et al., 2015). Both enzymes also interact with the exposed long DNA linker, and for INO80C, this appears to be due to an Actin-Arp subunit module (Act1/Arp4/Arp8 for INO80C). Interactions with linker DNA may help to recruit or orient SWR1C, or such contacts may prevent propagation of the DNA translocation event so that nucleosome positions are unchanged (Clapier et al., 2017).

Remarkably, binding of INO80C to the nucleosome releases ~15 bp of DNA from the histone octamer surface where the ATPase lobes interact at SHL-6 (Eustermann et al., 2018; Ayala et al., 2018). Likewise, cryo-EM analysis of the SWR1C-nucleosome complex indicates that nucleosome binding by SWR1C disrupts histone-DNA contacts at the linker-

distal nucleosome edge (SHL+6), with two subunits (Swc6 and Arp6) serving as a wedge that may help to displace DNA from the octamer surface (Willhoft et al., 2018). Importantly, this SWR1C-nucleosome complex was formed in the presence of both H2A.Z-H2B dimers and ADP-BeF_3, a putative ground-state nucleotide analog; thus, the structure may reflect a "snapshot" of the transient, unwrapped state we measured in ensemble FRET time courses.

Does DNA Translocation Promote Histone Replacement?

In the SWI2-SNF2 ATPase, DNA-stimulated ATPase activity has been attributed to a DNA-mediated rearrangement of the ATPase lobes that orients catalytic residues for ATP hydrolysis (Durr et al., 2005). Likewise, recent cryo-EM structures of Chd1-nucleosome and SWR1C-nucleosome complexes show that the two ATPase lobes of the remodeler undergo a well-pronounced structural change in the presence of a ADP-BeF_3 (Farnung et al., 2017; Willhoft et al., 2018), inducing close interactions with the nucleosome at the SHL2 region. For SWR1C, binding of ADP-BeF_3 appears to be sufficient for translocation of 1 bp of DNA toward the nucleosomal dyad (Willhoft et al., 2018). Interestingly, recent studies with the Chd1 remodeler also suggest that closure of the ATPase lobes is sufficient to induce a 1-bp translocation step (Winger et al., 2018). Consistent with this view, our studies demonstrate that the stimulation of ATP hydrolysis is eliminated by a 2-nt gap at SHL2, indicating that tracking of nucleosomal DNA is fine-tuned with the kinetic events of the ATPase cycle. Thus, intact nucleosomal DNA is likely to provide a macro-molecular context essential for optimum closure of the ATPase lobes upon ATP binding (Dürr et al., 2005; Farnung et al., 2017). Based on our FCS-FRET studies and recently published single molecule FRET (smFRET) results, this ATP-bound form of the SWR1C-nucleosome complex also shows enhanced dynamics of DNA-histone interactions at the nucleosomal edge. For SWR1C, only single-stranded DNA (ssDNA) gaps within the binding site at SHL2 block dimer exchange (±17 bp to ±23 bp from the nucleosomal dyad) (Ranjan et al., 2015), suggesting that SWR1C may only need to translocate a few base pairs. We envision that such limited DNA translocation may destabilize DNA between SHL2 and the nucleosome edge at SHL6, facilitating exposure of the H2A-H2B surface for DNA unwrapping by the Swc6/Arp6 wedge (Willhoft et al., 2018). In this model, our ensemble FRET assay measures the combined effects of DNA translocation and DNA unwrapping, resulting in transient loss of FRET concurrent with initial dimer eviction. Such a rapid but limited amount of DNA translocation may not only weaken histone-DNA contacts but also lead to allosteric changes in the histone octamer that destabilize the H2A-H2B and H3/H4 interface (Sinha et al., 2017).

SWR1C Catalyzes an Asymmetric Dimer Exchange Reaction

Previous gel-based assays for H2A.Z deposition demonstrated that the dimer exchange reaction is a sequential (Luk et al., 2010), stepwise process when assayed under steady-state assay conditions. We were surprised, however, to find that our single-turnover exchange reactions were clearly biphasic, with the first phase occurring at a rate about ~6-fold faster than the second phase. Furthermore, 2-nt DNA gaps at either SHL+2.0 or SHL2.0 produced monophasic kinetic profiles that maintained either the fast or slow rates observed with intact nucleosomes. These data suggest the intriguing possibility that SWR1C catalyzes two sequential rounds of dimer exchange without a requisite dissociation from the nucleosome

substrate. Furthermore, the slower rate of the second phase suggests that the second round of dimer exchange has a different rate-limiting step or an altered reaction pathway.

How might SWR1C accomplish this feat? We envision that, following exchange of the first H2A-H2B dimer, SWR1C must re-orient its ATPase lobes to the opposite DNA gyre so that it can initiate a DNA translocation event that unwraps the long linker DNA end, promoting eviction of the linker-proximal dimer. Importantly, re-orientation of the lobes would not require dissociation of the entire enzyme from the nucleosome. Intriguingly, a recent study has suggested that the Chd1 remodeling enzyme may re-orient its ATPase lobes back and forth between SHL2 and SHL6 during ATP-dependent nucleosome mobilization (Qiu et al., 2017). However, it seems unlikely that the SWR1C ATPase re-orients to SHL6 for the second round of dimer exchange because a gap at SHL2 blocks this second exchange reaction. More likely, there may be a more dramatic re-organization of the SWR1C ATPase lobes so that they engage SHL2 on the opposite DNA gyre. In this model, binding of the Actin-Arp module to the long linker DNA might stabilize the enzyme-nucleosome complex (Brahma et al., 2017; Eustermann et al., 2018; Ayala et al., 2018). Flexibility of the remodeler ATPase lobes for multiple, alternative interactions with nucleosomal DNA may be a hallmark of these enzymes.

From yeast to mammals, H2A.Z deposition appears to be targeted to the nucleosome adjacent to the start site for transcription by RNA polymerase II (Albert et al., 2007; Barski et al., 2007). Often termed the +1 nucleosome, it is inherently asymmetric, with one side flanked by an NDR of 140–250 bp and the other side by the +2 nucleosome, which can be separated from the +1 by less than 20 bp of linker DNA (Jiang and Pugh 2009). In yeast, targeting of SWR1C to the +1 nucleosome relies on protein-DNA interactions between SWR1C and the NDR region (Ranjan et al., 2013), whereas the related vertebrate enzymes, SRCAP and p400/Tip60, are believed to be recruited to promoter-proximal regions by gene-specific regulators (Pradhan et al., 2016). Our *in vitro* nucleosome substrate mimics the asymmetry of the +1 nucleosome because it is flanked by a 55- to 77-bp linker. Previous DNA footprinting studies have shown that interactions between SWR1C and the long linker DNA appear to orient the ATPase lobes of the Swr1 catalytic subunit to interact with linker-distal SHL+2.0 (Ranjan et al., 2015), and we found that this leads to the preferential eviction of the linker-distal H2A-H2B dimer in the initial, fast phase of the biphasic exchange reaction (Figure 3B). We note that a recent study did not observe such preferential exchange of the distal dimer, likely because of the fact that their nucleosomal substrate had relatively long linkers on both sides of the nucleosome (Willhoft et al., 2018).

Recent high-resolution ChIP-exo analyses of nucleosome asymmetry in yeast are fully consistent with asymmetric dimer exchange (Rhee et al., 2014). At the +1 nucleosome, the promoter-distal half of the nucleosome is highly enriched for H2A.Z, whereas the promoter-proximal side is enriched for H2A. Interestingly, the promoter-proximal side is also enriched for ubiquitinylated H2B (H2B-ub), a mark associated with active transcription (Rhee et al., 2014; Zhang 2003). One interesting possibility is that H2B-ub might enhance the intrinsic kinetic delay of the second round of dimer exchange, ensuring that the +1 nucleosome remains asymmetric with respect to H2A.Z deposition. In addition, our studies suggest that DNA sequence may also affect the rate of the second round of dimer exchange and, thus,

that asymmetric DNA sequences at promoter-proximal nucleosomes may also enhance the accumulation of H2A/H2A.Z heterotypic nucleosomes.

What might be the functional significance of dimer exchange asymmetry? We consider two possibilities that would be consistent with the known role of H2A.Z in promoting rapid induction of transcription from a poised promoter (Guillemette et al., 2005). First, there may be unique biochemical properties for a heterotypic H2A.Z/H2A nucleosome, especially when the H2A-H2B dimer contains a mono-ubiquitin mark. H2B-ub can disrupt nucleosome-nucleosome interactions *in vitro* (Fierz et al., 2011), and together with H2A.Z, this combination may favor subsequent nucleosome disruption during transcription initiation. Alternatively, the kinetic lag between the first and second rounds of dimer exchange may lead to an accumulation of a remodeling intermediate where SWR1C enhances the wrapping/unwrapping dynamics of nucleosomal DNA on the NDR-proximal side. In yeast, the NDR proximal side of the nucleosome often contains the site of transcription initiation (Jiang and Pugh 2009), and, thus, a mechanism that specifically enhances accessibility to this face of the nucleosome would be particularly advantageous.

STAR⋆METHODS

CONTACT FOR REAGENT AND RESOURCE SHARING

Further information and requests for resources and reagents should be directed to and will be fulfilled by the Lead Contact, Craig Peterson (Craig.Peterson@umassmed.edu).

EXPERIMENTAL MODEL AND SUBJECT DETAILS

Bacterial Strains—E.coli strains Rosetta(DE3)pLysS (Novagen) and Rosetta 2 (Novagen) were used for histone expression. Cells were grown in standard LB media at 37°C.

Yeast Strains—Strain W1588–4C (MATa *ade2–1 can1–100 his3–11,15 leu2–3,112 trp1–1 ura3–1 RAD5+ swr1::SWR1–3xFLAG-P-KanMX-P htz1::natMX4*) was used for purification of SWR1C. Yeast were grown in YEPD media, supplemented with adenine, at 30°C until an OD_{600} of 3–6.

METHOD DETAILS

Reconstitution of fluorescently labeled mononucleosomes—Recombinant Saccharomyces cerevisiae (H2A, H2A.Z, H2B, H3, and H4) and *Xenopus laevis* or human histones (H3 and H4) were expressed in *Escherichia coli* (Rosetta 2(DE3)pLysS for all histones, except for histone H4 which used Rosetta 2) and purified from inclusion bodies as described previously (Luger et al., 1999). The unique cysteine substitutions were introduced at H2A-119 and H3–33 using site-directed mutagenesis. Histones were labeled with Cy5 and Cy3 using maleimide chemistry and reconstituted into dimers and octamers as described previously (Zhou and Narlikar, 2016; Luger et al., 1999). The purified, concentrated dimer and octamer stocks were diluted 1:1 with freeze buffer (10 mM Tris-HCl, pH = 7.4, 2 M NaCl, 40% glycerol, 5 mM β-Mercaptoethanol), aliquoted, flash frozen, and stored at −80°C for nucleosome reconstitution and dimer exchange assays. Cy3-labeled DNA fragments containing an end-positioned 601 nucleosome positioning sequence or unlabeled, center-

positioned 601 DNA fragments were prepared by PCR amplification using 500nM of 5′Cy3-conjugated or unlabeled PCR primers purchased from IDT, 0.1 ng/ul pGEM-601 plasmid, 200 uM dNTPs, and either 0.02 U/ul Phusion DNA polymerase in 1× Phusion High Fidelity Buffer or 0.025 U/ul Taq DNA polymerase in 1× ThermoPol Buffer under the recommended conditions from NEB (Phusion: https://www.neb.com/protocols/1/01/01/pcr-protocol-m0530; ThermoPol Taq: https://www.neb.com/protocols/1/01/01/taq-dna-polymerase-with-thermopol-buffer-m0267). The PCR products were purified using a Zymo DNA Clean & Concentrator kit and concentrated by ethanol precipitation. Fluorescent mononucleosomes were reconstituted at 300–600 nM concentration via salt gradient dialysis (Luger et al., 1999), dialyzing in 600 mL of high buffer (10 mM Tris-HCl, pH = 7.4, 1 mM EDTA, 2M KCl, 1 mM DTT), exchanged with 3 L of low buffer (10 mM Tris-HCl, pH = 7.4, 1 mM EDTA, 50 mM KCl, 1 mM DTT) over 20 hr at 4°C using a peristaltic pump. For each set of reconstitutions, at least three different ratios of histone octamer to DNA template, close to 1:1 were assembled, visualized on a 4.5% native-PAGE gel via SYBR Gold (Thermo Fisher Scientific) staining or Cy3/Cy5 fluorescence using a Typhoon Imager (GE), and the reconstitution that yielded 1%–5% free DNA was chosen for subsequent reactions. The gapped mononucleosomes were reconstituted using the 202 bp DNA fragment containing the end-positioned 601 positioning sequence harboring 2nt gap at the SHL ± 2 region. The gapped DNA fragment was generated by PCR amplification using primers that contain deoxyuridine bases at the specific gap sites. In order to create a gap in the above PCR product, it was treated with USER enzyme – a mixture of DNA glycosylase and endonuclease III. The complete removal of deoxyuridine from the PCR product by USER enzyme was confirmed upon its treatment with S1 nuclease.

Purification of yeast SWR1C—SWR1C was purified from whole cell extracts of a *S. cerevisiae* strain harboring a FLAG-tagged allele of the Swr1 ATPase (Swr1–3xFLAG) as detailed elsewhere (Mizuguchi et al., 2012) with the following modifications: A PM 100 cryomill was used to lyse the harvested yeast noodles with 6 × 1 min cycles at 400 rpm. During affinity purification of SWR1C, the MNase digestion step was skipped. Following FLAG peptide elution, SWR1C was either aliquoted, flash frozen, and stored in B-0.1 buffer (25 mM HEPES, pH = 7.6, 1 mM EDTA, 2 mM $MgCl_2$, 10 mM β-glycerophosphate, 1 mM Na-butyrate, 0.5 mM NaF, 100 mM KCl, 10% glycerol, 0.05% Tween-20) with 0.5 mg/mL FLAG peptide at −80°C for future use, or further purified on a 5 ml, 5%–30% glycerol gradient in buffer D (25 mM HEPES, pH = 7.6, 1 mM EDTA, 2 mM $MgCl_2$, 100 mM KCl). Gradients were sedimented for 14 hours at 35,000 rpm, collected in 200 ul fractions, and imaged by SDS-PAGE and silver staining. Peak fractions of SWR1C were pooled, concentrated using a 10 kDa cutoff Amicon Ultra-0.5 mL centrifugal filter (Millipore), and dialyzed overnight against storage buffer (25 mM HEPES, pH = 7.6, 1 mM EDTA, 2 mM $MgCl_2$, 100 mM KCl, and 10% glycerol). Concentrated SWR1C was aliquoted, flash frozen, and stored at −80°C. SWR1C concentration was determined by SDS-PAGE using a BSA (NEB) standard titration, followed by SYPRO Ruby (Thermo Fisher Scientific) staining and quantification using ImageQuant 1D gel analysis.

Nucleosome dynamics measurements using fluorescence correlation spectroscopy (FCS)—FCS measurements were carried out using an in-house automated

FCS set up. Excitation was provided by a 488 nm single-mode fiber coupled picosecond diode laser (BDL-488-SMN, Becker & Hickl GmBH) that was expanded to overfill the microscope objective. The excitation was focused on the sample and collected by an Olympus UPlanSApo 60× 1.2 N.A. water immersion objective. The collected light was focused on a 50-micron pinhole and then further collimated and split into a donor (Cy3) and acceptor (Cy5) channel using a dichroic beamsplitter. Additional bandpass filters were placed before the detectors. Single-photon avalanche photodiodes (SPAD) (ID100–50, low-noise, ID Quantique, Switzerland) were used for detection. The output of the SPADs were inverted and directed into a time-correlated single-photon counting card (SPC150, Becker & Hickl GmBH). Samples were placed in 170-micron glass coverslip bottom 96-well microplates (Greiner Bio-One). Autofocusing and fully automated data collection were enabled by a custom computer-controlled, microplate-compatible x-y-z stage. A Microlab titrator (Microlab 500, Hamilton Company) automatically added immersion water to the objective prior to each acquisition. Each FCS trace was the result of 10 × 300 s collections. FCS experiments were performed using 10 nM nucleosome bearing the FRET donor-acceptor pair in remodeling buffer (25 mM HEPES, pH = 7.6, 0.2 mM EDTA, 5 mM MgCl2, 70 mM KCl, 1 mM DTT). SWR1C was dialyzed overnight against the remodeling buffer prior to use in the FCS experiments. The FCS measurements of the nucleosome in the presence SWR1C and ATP analog AMP-PNP were performed under saturating enzyme and nucleotide concentrations. The acceptor autocorrelation function (GAA) and the donor/acceptor cross-correlation function (GDA) were determined using the Burst Analyzer software package. Since the relaxation time of the conformational fluctuation (observed rate constant, *kobs*) of the nucleosome can be derived from the ratio of any two correlation functions (Tims et al., 2011; Torres and Levitus, 2007), we utilized the values of GDA/GAA to obtain the kinetic parameters associated with conformational fluctuation of the nucleosome under various experimental conditions. The characteristic exponential curves associated with the ratio of two correlation functions (GDA/GAA) were analyzed using a single/double exponential rate equation, yielding the kobs values of the conformational fluctuation of the nucleosome.

Transient kinetic measurements of nucleosome remodeling—The transient kinetic experiments of the SWR1C-catalyzed nucleosome remodeling reaction were carried out under single turnover conditions (excess SWR1C over nucleosome). Nucleosomes were assembled either with a yeast histone octamer or a yeast/*X. laevis*/human hybrid octamer where the histone H3/H4 tetramer contained *X. laevis* H4 and human H3.2. Hybrid nucleosomes were only used for assays that employed an H3-Cy5 label, as this labeling position differentially de-stabilized the yeast octamer. Notably, the biphasic rates of dimer eviction were identical between yeast and hybrid substrates (Figure S4C). The time-dependent fluorescence measurements during the SWR1C-catalyzed nucleosome reaction as well as pre-and post-reaction emission spectral scans were carried out using an ISS PC1 spectrofluorometer or a Tecan Infinite M1000 PRO microplate reader. The nucleosome remodeling reactions were performed in remodeling buffer (25 mM HEPES, pH = 7.6, 0.2 mM EDTA, 5 mM $MgCl_2$, 70 mM KCl, 1 mM DTT) at room temperature. A representative nucleosome remodeling reaction contained 50–100 ul of 10 nM nucleosome (bearing FRET pair), at least 2.5-fold excess of SWR1C, and 200 uM-1 mM ATP or AMP-AMP. In order to

monitor dimer exchange, a two- to seven-fold excess concentration of H2A.Z-H2B dimer relative to the nucleosome was used. The nucleosome was incubated with SWR1C in the presence or absence of the H2A.Z-H2B dimer for 5 min at room temperature to synchronize/pre-equilibrate the nucleosome-remodeler complex. The remodeling reaction was started with the addition of ATP or AMP-PNP. In the no enzyme controls, equivalent volume of SWR1C elution buffer containing 0.5 mg/mL FLAG peptide was added instead. At least 2–4 kinetic traces were collected for each dataset and averaged to enhance the signal to noise ratio. The transient kinetic parameters of the SWR1C-catalyzed nucleosome reaction were obtained from the time-dependent change in the Cy5 FRET signal at 670nm upon 530nm excitation. The averaged kinetic traces associated with the nucleosome remodeling reaction were analyzed using single and double exponential rate equations as described below yielding the k_{obs} values associated with the respective remodeling reaction.

$$\mathrm{RFU} = \mathrm{A}e^{-kobs\,.\,t} + \mathrm{offset}$$

$$\mathrm{RFU} = \mathrm{A}_1 e^{-kobs1.t} + \mathrm{A}_2 e^{-kobs2.t} + \mathrm{offset}$$

In the above equations, RFU is relative fluorescence signal, A is the associated amplitude of the fluorescence signal, k_{obs} is the observed rate constant, t is the time, and the *offset* is the end point of the fluorescence signal. All curve fittings were performed in the OriginLab software package and the standard error associated with the parameters obtained upon fitting have been reported.

ATPase ASSAYS—The real-time and direct measurement of inorganic phosphate (P_i) was performed using a phosphate sensor, which is 7-Diethylamino-3-[N-(2-maleimidoethyl)carbamoyl]coumarin conjugated to phosphate-binding protein A197C (PBP-MDCC) (Brune et al., 1994). Precise measurements of the pre-steady state kinetic parameters of SWR1C-catalyzed ATP hydrolysis were unsuccessful even at reduced temperature (4°C) and lower concentration of ATP, which were used to slow down the ATPase activity (for reliable rate measurements) and reduce the amount of free phosphate ion present in the ATP solution, respectively. In view of the above experimental limitation, we performed the steady-state kinetic analysis of the SWR1C-catalyzed ATP hydrolysis by discarding data points from the initial 300 s. The experimental conditions used in the ATPase assay were as follows: [SWR1C] = 5 nM, [ATP] = 100 μM, [H2A-nucleosome] = 10 μM, [PBP-MDCC] = 2 μM, [H2A.Z-H2B dimer] = 20 nM. The real-time monitoring of P_i produced during the SWR1C-catalyzed reaction was performed on ISS PC1 spectrofluorometer upon exciting the sample at 425 nm and monitoring emission at 460 nm. At least 3–4 kinetic traces were averaged and analyzed using the steady-state equation as described below (Fersht, 1999),

$$\mathrm{V}_0 = k_{\mathrm{cat}}/K_{\mathrm{m}}[\mathrm{E}][\mathrm{S}]$$

where V_0 is the rate of ATP hydrolysis by SWR1C, k_{cat} is the rate constant of hydrolysis, K_m is the Michaelis constant, [E] is the concentration of SWR1C, and [S] is the concentration of ATP. The amount of Pi produced during the steady-state of SWR1C-catalyzed ATP hydrolysis was calculated using the linear standard curve of Pi.

QUANTIFICATION AND STATISTICAL ANALYSES

At least 10–15 FCS traces were collected, and the Cy3 and Cy5 photon counts signal were auto and cross-correlated in 300 s cycles using Burst Analyzer. The correlation curves were averaged and fitted with the single and double exponential rate equation as described below. Non-linear regression analysis was performed using Origin Software package to obtain the line of best fit. The standard *error* associated with the parameters and the *reduced Chi-square* derived upon curve fitting were used as to measure the precision of fitted value.

In order to enhance the robustness of the quantitative measurement in the nucleosome remodeling reactions, the random noise was reduced by averaging at least 3–4 kinetic traces. The averaged traces were analyzed using single and double exponential rate equations as described below yielding the k_{obs} values associated with the respective remodeling reaction.

$$\mathrm{RFU} = \mathrm{A}e^{-kobs\,.\,t} + \mathrm{offset}$$

$$\mathrm{RFU} = \mathrm{A}_1 e^{-kobs1.t} + \mathrm{A}_2 e^{-kobs2.t} + \mathrm{offset}$$

In the above equations, RFU is relative fluorescence signal, A is the associated amplitude of the fluorescence signal, k_{obs} is the observed rate constant, t is the time, and the *offset* is the end point of the fluorescence signal. All curve fittings were performed in the OriginLab software package and, the precision of the fitted parameters was evaluated using the associated *standard error* and the *Reduced Chi-square* values.

Supplementary Material

Refer to Web version on PubMed Central for supplementary material.

ACKNOWLEDGMENTS

We thank members of the Peterson lab for helpful discussions, Yonca Karadeniz for providing some of the SWR1C for this study, and Salih Topal for help with the graphical abstract. We also thank David Lambright (UMMS) for access to his ISS PC1 spectrofluorometer. This work was supported by grants from the NIH (GM049650 and GM122519 to C.L.P.) and a postdoctoral fellowship from the American Heart Association (to R.K.S.).

REFERENCES

Adkins NL, Niu H, Sung P, and Peterson CL (2013). Nucleosome dynamics regulates DNA processing. Nat. Struct. Mol. Biol 20, 836–842. [PubMed: 23728291]

Agarwal PK, Billeter SR, Rajagopalan PTR, Benkovic SJ, and Hammes-Schiffer S (2002). Network of coupled promoting motions in enzyme catalysis. Proc. Natl. Acad. Sci. USA 99, 2794–2799. [PubMed: 11867722]

Albert I, Mavrich TN, Tomsho LP, Qi J, Zanton SJ, Schuster SC, and Pugh BF (2007). Translational and rotational settings of H2A.Z nucleosomes across the Saccharomyces cerevisiae genome. Nature 446, 572–576. [PubMed: 17392789]

Ayala R, Willhoft O, Aramayo RJ, Wilkinson M, McCormack EA, Ocloo L, Wigley DB, and Zhang X (2018). Structure and regulation of the human INO80-nucleosome complex. Nature 556, 391–395. [PubMed: 29643506]

Banaszynski LA, Allis CD, and Lewis PW (2010). Histone variants in metazoan development. Dev. Cell 19, 662–674. [PubMed: 21074717]

Barski A, Cuddapah S, Cui K, Roh T-Y, Schones DE, Wang Z, Wei G, Chepelev I, and Zhao K (2007). High-resolution profiling of histone methylations in the human genome. Cell 129, 823–837. [PubMed: 17512414]

Benkovic SJ, and Hammes-Schiffer S (2003). A perspective on enzyme catalysis. Science 301, 1196–1202. [PubMed: 12947189]

Bowman GD (2010). Mechanisms of ATP-dependent nucleosome sliding. Curr. Opin. Struct. Biol 20, 73–81. [PubMed: 20060707]

Brahma S, Udugama MI, Kim J, Hada A, Bhardwaj SK, Hailu SG, Lee T-H, and Bartholomew B (2017). INO80 exchanges H2A.Z for H2A by translocating on DNA proximal to histone dimers. Nat. Commun 8, 15616. [PubMed: 28604691]

Brune M, Hunter JL, Corrie JE, and Webb MR (1994). Direct, real-time measurement of rapid inorganic phosphate release using a novel fluorescent probe and its application to actomyosin subfragment 1 ATPase. Biochemistry 33, 8262–8271. [PubMed: 8031761]

Cairns BR (2009). The logic of chromatin architecture and remodelling at promoters. Nature 461, 193–198. [PubMed: 19741699]

Clapier CR, Iwasa J, Cairns BR, and Peterson CL (2017). Mechanisms of action and regulation of ATP-dependent chromatin-remodelling complexes. Nat. Rev. Mol. Cell Biol 18, 407–422. [PubMed: 28512350]

Daniel RM, Dunn RV, Finney JL, and Smith JC (2003). The role of dynamics in enzyme activity. Annu. Rev. Biophys. Biomol. Struct 32, 69–92. [PubMed: 12471064]

Dion MF, Kaplan T, Kim M, Buratowski S, Friedman N, and Rando OJ (2007). Dynamics of replication-independent histone turnover in budding yeast. Science 315, 1405–1408. [PubMed: 17347438]

Dürr H, Körner C, Müller M, Hickmann V, and Hopfner K-P (2005). X-ray structures of the Sulfolobus solfataricus SWI2/SNF2 ATPase core and its complex with DNA. Cell 121, 363–373. [PubMed: 15882619]

Eisenmesser EZ, Bosco DA, Akke M, and Kern D (2002). Enzyme dynamics during catalysis. Science 295, 1520–1523. [PubMed: 11859194]

Eustermann S, Schall K, Kostrewa D, Lakomek K, Strauss M, Moldt M, and Hopfner K-P (2018). Structural basis for ATP-dependent chromatin remodelling by the INO80 complex. Nature 556, 386–390. [PubMed: 29643509]

Faast R, Thonglairoam V, Schulz TC, Beall J, Wells JRE, Taylor H, Matthaei K, Rathjen PD, Tremethick DJ, and Lyons I (2001). Histone variant H2A.Z is required for early mammalian development. Curr. Biol 11, 1183–1187. [PubMed: 11516949]

Fan JY, Gordon F, Luger K, Hansen JC, and Tremethick DJ (2002). The essential histone variant H2A.Z regulates the equilibrium between different chromatin conformational states. Nat. Struct. Biol 9, 172–176. [PubMed: 11850638]

Farnung L, Vos SM, Wigge C, and Cramer P (2017). Nucleosome-Chd1 structure and implications for chromatin remodelling. Nature 550, 539–542. [PubMed: 29019976]

Fersht A (1999). Structure and Mechanism in Protein Science: A Guide to Enzyme Catalysis and Protein Folding (Freeman).

Feynman RP, and Sands LM (1963). The Feynman Lectures on Physics (Addison-Wesley).

Fierz B, Chatterjee C, McGinty RK, Bar-Dagan M, Raleigh DP, and Muir TW (2011). Histone H2B ubiquitylation disrupts local and higher-order chromatin compaction. Nat. Chem. Biol 7, 113–119. [PubMed: 21196936]

Gévry N, Chan HM, Laflamme L, Livingston DM, and Gaudreau L (2007). p21 transcription is regulated by differential localization of histone H2A.Z. Genes Dev. 21, 1869–1881. [PubMed: 17671089]

Guillemette B, Bataille AR, Gévry N, Adam M, Blanchette M, Robert F, and Gaudreau L (2005). Variant histone H2A.Z is globally localized to the promoters of inactive yeast genes and regulates nucleosome positioning. PLoS Biol. 3, e384. [PubMed: 16248679]

Hammes GG (2002). Multiple conformational changes in enzyme catalysis. Biochemistry 41, 8221–8228. [PubMed: 12081470]

Hartley PD, and Madhani HD (2009). Mechanisms that specify promoter nucleosome location and identity. Cell 137, 445–458. [PubMed: 19410542]

Henikoff S (2016). Mechanisms of Nucleosome Dynamics In Vivo. Cold Spring Harb. Perspect. Med 6, a026666. [PubMed: 27503998]

Henzler-Wildman K, and Kern D (2007). Dynamic personalities of proteins. Nature 450, 964–972. [PubMed: 18075575]

Henzler-Wildman KA, Lei M, Thai V, Kerns SJ, Karplus M, and Kern D (2007). A hierarchy of timescales in protein dynamics is linked to enzyme catalysis. Nature 450, 913–916. [PubMed: 18026087]

Hong J, Feng H, Wang F, Ranjan A, Chen J, Jiang J, Ghirlando R, Xiao TS, Wu C, and Bai Y (2014). The catalytic subunit of the SWR1 remodeler is a histone chaperone for the H2A.Z-H2B dimer. Mol. Cell 53, 498–505. [PubMed: 24507717]

Jencks WP (1989). How does a calcium pump pump calcium? J. Biol. Chem 264, 18855–18858. [PubMed: 2530226]

Jiang C, and Pugh BF (2009). Nucleosome positioning and gene regulation: advances through genomics. Nat. Rev. Genet 10, 161–172. [PubMed: 19204718]

Kobor MS, Venkatasubrahmanyam S, Meneghini MD, Gin JW, Jennings JL, Link AJ, Madhani HD, and Rine J (2004). A protein complex containing the conserved Swi2/Snf2-related ATPase Swr1p deposits histone variant H2A.Z into euchromatin. PLoS Biol. 2, E131. [PubMed: 15045029]

Li G, and Widom J (2004). Nucleosomes facilitate their own invasion. Nat. Struct. Mol. Biol 11, 763–769. [PubMed: 15258568]

Li G, Levitus M, Bustamante C, and Widom J (2005). Rapid spontaneous accessibility of nucleosomal DNA. Nat. Struct. Mol. Biol 12, 46–53. [PubMed: 15580276]

Luger K, Mäder AW, Richmond RK, Sargent DF, and Richmond TJ (1997). Crystal structure of the nucleosome core particle at 2.8 A resolution. Nature 389, 251–260. [PubMed: 9305837]

Luger K, Rechsteiner TJ, and Richmond TJ (1999). Preparation of nucleosome core particle from recombinant histones. Methods Enzymol. 304, 3–19. [PubMed: 10372352]

Luk E, Ranjan A, Fitzgerald PC, Mizuguchi G, Huang Y, Wei D, and Wu C (2010). Stepwise histone replacement by SWR1 requires dual activation with histone H2A.Z and canonical nucleosome. Cell 143, 725–736. [PubMed: 21111233]

Meneghini MD, Wu M, and Madhani HD (2003). Conserved histone variant H2A.Z protects euchromatin from the ectopic spread of silent heterochromatin. Cell 112, 725–736. [PubMed: 12628191]

Mizuguchi G, Shen X, Landry J, Wu W-H, Sen S, and Wu C (2004). ATP-driven exchange of histone H2AZ variant catalyzed by SWR1 chromatin remodeling complex. Science 303, 343–348. [PubMed: 14645854]

Mizuguchi G, Wu W-H, Alami S, and Luk E (2012). Biochemical assay for histone H2A.Z replacement by the yeast SWR1 chromatin remodeling complex. Methods Enzymol. 512, 275–291. [PubMed: 22910211]

Nashine VC, Hammes-Schiffer S, and Benkovic SJ (2010). Coupled motions in enzyme catalysis. Curr. Opin. Chem. Biol 14, 644–651. [PubMed: 20729130]

Ngo TT, Zhang Q, Zhou R, Yodh JG, and Ha T (2015). Asymmetric unwrapping of nucleosomes under tension directed by DNA local flexibility. Cell 160, 1135–1144. [PubMed: 25768909]

Park YJ, Dyer PN, Tremethick DJ, and Luger K (2004). A new fluorescence resonance energy transfer approach demonstrates that the histone variant H2AZ stabilizes the histone octamer within the nucleosome. J. Biol. Chem 279, 24274–24282. [PubMed: 15020582]

Pradhan SK, Su T, Yen L, Jacquet K, Huang C, Co^té J, Kurdistani SK, and Carey MF (2016). EP400 Deposits H3.3 into Promoters and Enhancers during Gene Activation. Mol. Cell 61, 27–38. [PubMed: 26669263]

Qiu Y, Levendosky RF, Chakravarthy S, Patel A, Bowman GD, and Myong S (2017). The Chd1 Chromatin Remodeler Shifts Nucleosomal DNA Bidirectionally as a Monomer. Mol. Cell 68, 76–88.e6. [PubMed: 28943314]

Raisner RM, Hartley PD, Meneghini MD, Bao MZ, Liu CL, Schreiber SL, Rando OJ, and Madhani HD (2005). Histone variant H2A.Z marks the 5′ ends of both active and inactive genes in euchromatin. Cell 123, 233–248. [PubMed: 16239142]

Ranjan A, Mizuguchi G, FitzGerald PC, Wei D, Wang F, Huang Y, Luk E, Woodcock CL, and Wu C (2013). Nucleosome-free region dominates histone acetylation in targeting SWR1 to promoters for H2A.Z replacement. Cell 154, 1232–1245. [PubMed: 24034247]

Ranjan A, Wang F, Mizuguchi G, Wei D, Huang Y, and Wu C (2015). H2A histone-fold and DNA elements in nucleosome activate SWR1-mediated H2A.Z replacement in budding yeast. eLife 4, e06845. [PubMed: 26116819]

Rhee HS, Bataille AR, Zhang L, and Pugh BF (2014). Subnucleosomal structures and nucleosome asymmetry across a genome. Cell 159, 1377–1388. [PubMed: 25480300]

Ruhl DD, Jin J, Cai Y, Swanson S, Florens L, Washburn MP, Conaway RC, Conaway JW, and Chrivia JC (2006). Purification of a human SRCAP complex that remodels chromatin by incorporating the histone variant H2A.Z into nucleosomes. Biochemistry 45, 5671–5677. [PubMed: 16634648]

Santisteban MS, Kalashnikova T, and Smith MM (2000). Histone H2A.Z regulates transcription and is partially redundant with nucleosome remodeling complexes. Cell 103, 411–422. [PubMed: 11081628]

Sauer RT, and Baker TA (2011). AAA+ proteases: ATP-fueled machines of protein destruction. Annu. Rev. Biochem 80, 587–612. [PubMed: 21469952]

Sinha KK, Gross JD, and Narlikar GJ (2017). Distortion of histone octamer core promotes nucleosome mobilization by a chromatin remodeler. Science 355, eaaa3761. [PubMed: 28104838]

Swygert SG, and Peterson CL (2014). Chromatin dynamics: interplay between remodeling enzymes and histone modifications. Biochim. Biophys. Acta 1839, 728–736. [PubMed: 24583555]

Tims HS, Gurunathan K, Levitus M, and Widom J (2011). Dynamics of nucleosome invasion by DNA binding proteins. J. Mol. Biol 411, 430–448. [PubMed: 21669206]

Torres T, and Levitus M (2007). Measuring conformational dynamics: a new FCS-FRET approach. J. Phys. Chem. B 111, 7392–7400. [PubMed: 17547447]

Vendruscolo M, and Dobson CM (2006). Structural biology. Dynamic visions of enzymatic reactions. Science 313, 1586–1587. [PubMed: 16973868]

Venkatesh S, and Workman JL (2015). Histone exchange, chromatin structure and the regulation of transcription. Nat. Rev. Mol. Cell Biol 16, 178–189. [PubMed: 25650798]

Watanabe S, Tan D, Lakshminarasimhan M, Washburn MP, Hong E-J, Walz T, and Peterson CL (2015). Structural Analyses of the chromatin remodeling enzymes INO80-C and SWR-C. Nat. Commun 6, 7108. [PubMed: 25964121]

Willhoft O, Ghoneim M, Lin C-L, Chua EYD, Wilkison M, Chaban Y, Ayala R, McCormack EA, Ocloo L, Rueda DS, and Wigley D (2018). Structure and dynamics of the yeast SWR1-nucleosome complex. Science 362, eaat7716. [PubMed: 30309918]

Winger J, and Bowman GD (2017). The sequence of nucleosomal DNA modulates sliding by the Chd1 chromatin remodeler. J. Mol. Biol 429, 808–822. [PubMed: 28189426]

Winger J, Nodelman IM, Levendosky RF, and Bowman GD (2018). A twist defect mechanism for ATP-dependent translocation of nucleosomal DNA. eLife 7, e34100. [PubMed: 29809147]

Wu WH, Alami S, Luk E, Wu CH, Sen S, Mizuguchi G, Wei D, and Wu C (2005). Swc2 is a widely conserved H2AZ-binding module essential for ATP-dependent histone exchange. Nat. Struct. Mol. Biol 12, 1064–1071. [PubMed: 16299513]

Xu Y, Ayrapetov MK, Xu C, Gursoy-Yuzugullu O, Hu Y, and Price BD (2012). Histone H2A.Z controls a critical chromatin remodeling step required for DNA double-strand break repair. Mol. Cell 48, 723–733. [PubMed: 23122415]

Yildirim O, Li R, Hung J-H, Chen PB, Dong X, Ee L-S, Weng Z, Rando OJ, and Fazzio TG (2011). Mbd3/NURD complex regulates expression of 5-hydroxymethylcytosine marked genes in embryonic stem cells. Cell 147, 1498–1510. [PubMed: 22196727]

Yuan G-C, Liu Y-J, Dion MF, Slack MD, Wu LF, Altschuler SJ, and Rando OJ (2005). Genome-scale identification of nucleosome positions in S. cerevisiae. Science 309, 626–630. [PubMed: 15961632]

Zhang Y (2003). Transcriptional regulation by histone ubiquitination and deubiquitination. Genes Dev. 17, 2733–2740. [PubMed: 14630937]

Zhou CY, and Narlikar GJ (2016). Analysis of nucleosome sliding by ATP-dependent chromatin remodeling enzymes. Methods Enzymol. 573, 119–135. [PubMed: 27372751]

Zhou CY, Johnson SL, Gamarra NI, and Narlikar GJ (2016). Mechanisms of ATP-Dependent Chromatin Remodeling Motors. Annu. Rev. Biophys 45, 153–181. [PubMed: 27391925]

Highlights

- SWR1C catalyzes two cycles of H2A.Z deposition by a biphasic, asymmetric reaction
- Binding of SWR1C enhances nucleosome dynamics
- Initial eviction of an H2A-H2B dimer involves ATP-dependent histone-DNA unwrapping
- Nucleosomal DNA sequence can modulate the rate of H2A.Z exchange

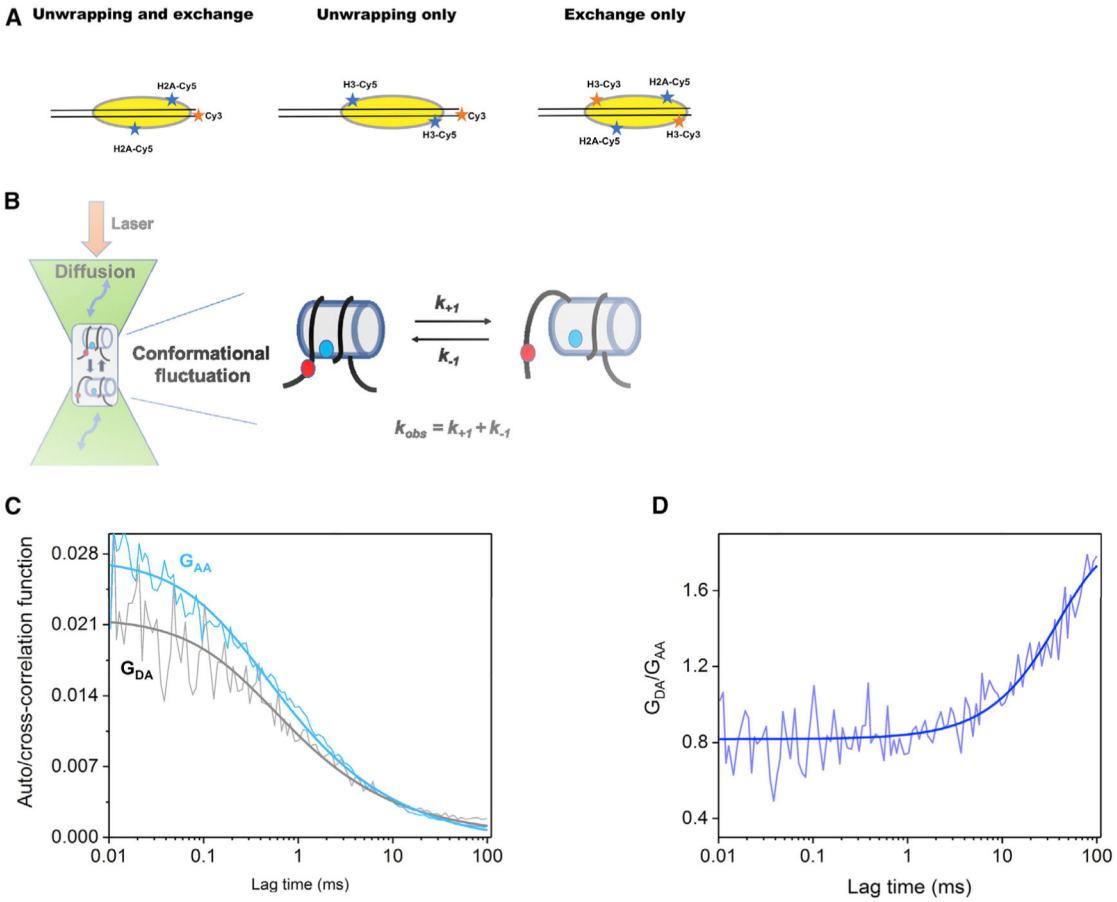

Figure 1. Conformational Fluctuations of the Nucleosome by FRET-FCS

(A) Nucleosomal FRET substrates. Red stars denote the location of the Cy3 donor, and blue stars denote the position of the Cy5 acceptor.

(B) Experimental setup for FCS-FRET using the H2A-Cy5/DNA-Cy3 substrate. A femtoliter volume of nucleosome solution is excited by a laser at the donor excitation wavelength. Fluctuations in donor and acceptor fluorescence signals are due to two events: (1) diffusion in and out of the confocal volume and (2) nucleosome conformational fluctuations that are dictated by the intrinsic microscopic rate constants (k_{+1} and k_{-1}), causing a distance change between the donor-acceptor pair (right image).

(C) The autocorrelation and cross-correlation functions of the acceptor and the donor-acceptor pair of the same nucleosome as a function of time are shown ascyan and black traces, respectively.

(D) The ratio of the two correlation functions as a function of time. The observed rate constant (k_{obs}) of the conformational fluctuation is obtained from the exponential fit of the ratio curve of these two correlation functions.

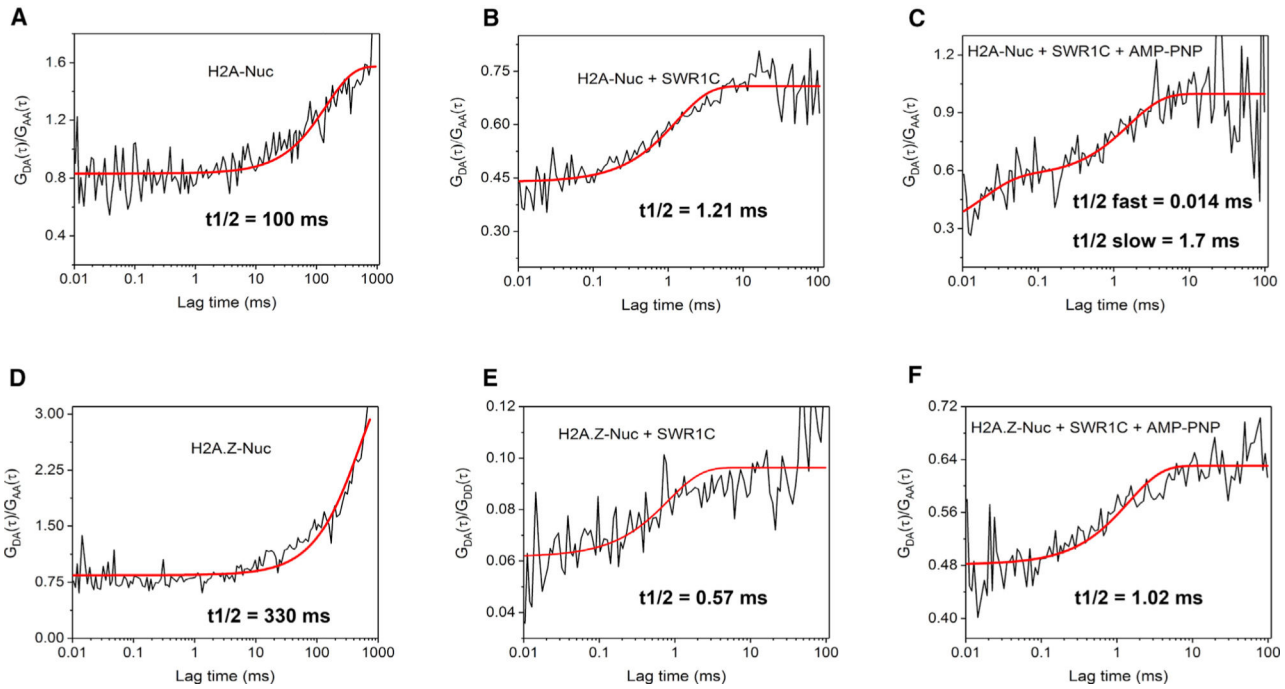

Figure 2. SWR1C Modulates the Conformational Fluctuations of the Nucleosome

(A–F) The ratios of donor-acceptor cross-correlation to acceptor auto-correlation are plotted as a function of time under various experimental conditions. The experimental data were analyzed using either a single- or double-exponential rate equation, yielding the values of the k_{obs} ($t_{1/2} = 0.693/k_{obs}$) for the conformational fluctuation of the nucleosome.

(A) Dynamics of an H2A-nucleosome.

(B) The dynamics of the SWR1C-H2A nucleosome complex are 2 orders of magnitude faster than the free nucleosome.

(C) Addition of AMP-PNP (a non-hydrolyzable analog of ATP) to the SWR1C-nucleosome complex induces additional nucleosome dynamics on the microsecond timescale.

(D) Dynamics of the H2A.Z nucleosome.

(E) The dynamics of the SWR1C-H2A.Z nucleosome complex are 2 orders of magnitude faster than the free nucleosome.

(F) Addition of AMP-PNP to the SWR1C-H2A.Z nucleosome does not alter nucleosome dynamics.

FCS curves were obtained after averaging at least 20–25 autocorrelation/cross-correlation curves.

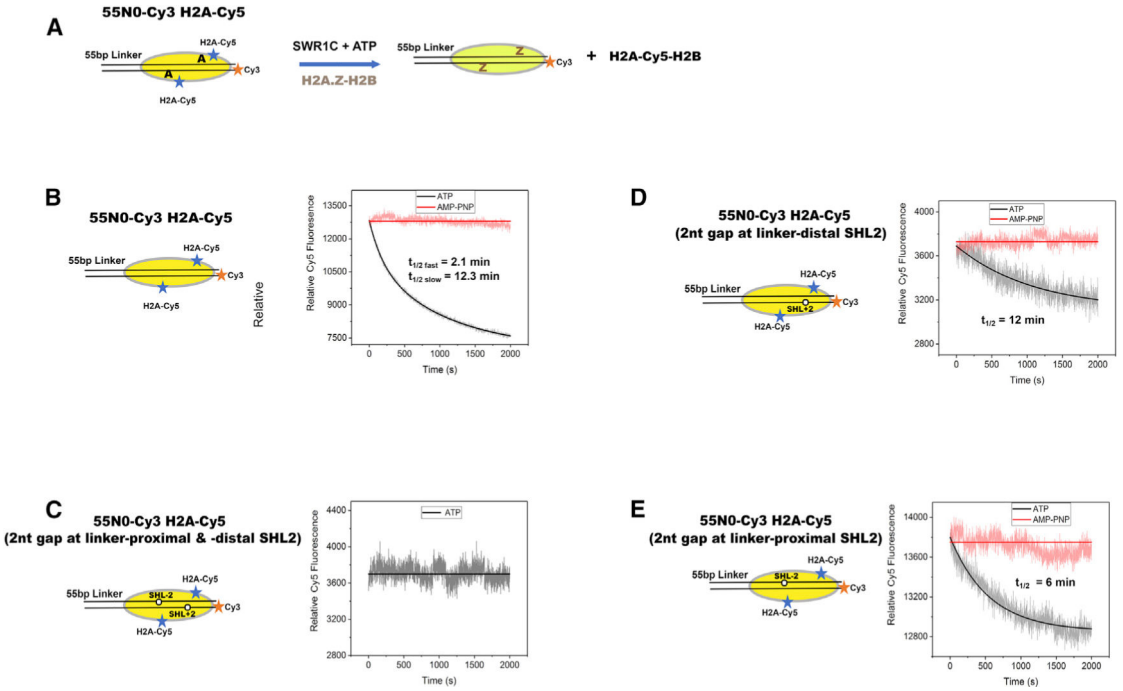

Figure 3. Transient Kinetics of ATP-Dependent Eviction of Two H2A-H2B Dimers from an H2A Nucleosome Are Asymmetric

(A) Experimental strategy for monitoring the rate of eviction of nucleosomal H2A-H2B. The nucleosomal substrate contains a Cy3-labeled DNA end, and Cy5 is located on the H2A C terminus. Cy5 FRET signals were monitored over time in reactions that contained free H2A.Z-H2B dimers.

(B) Representative kinetic trace for SWR1C-catalyzed eviction of H2A-H2B dimers from an H2A nucleosome. The experimental data were analyzed using adouble-exponential rate equation, yielding the k_{obs} for the fast and slow phases as 0.33 ± 0.02 min^{-1} (half-life = 2.1 min) and 0.06 ± 0.01 min^{-1}(half-life = 12.3 min), respectively.

(C) The kinetic trace for SWR1C-catalyzed eviction of H2A-H2B dimers from an H2A nucleosome containing a 2-nt gap at both SHL+2.0 and SHL−2.0.

(D) The kinetic trace for SWR1C-catalyzed eviction of the H2A-H2B dimer from an H2A nucleosome harboring a 2-nt gap at the linker-distal SHL+2.0. The monophasic trace was analyzed using a single-exponential rate equation, yielding the k_{obs} as 0.06 ± 0.01 min^{-1}(half-life = 12 min).

(E) The kinetic trace for SWR1C-catalyzed eviction of the H2A-H2B dimer from an H2A nucleosome harboring a 2-nt gap at the linker-proximal SHL−2.0. The kinetic trace is monophasic; hence, it was analyzed using a single-exponential rate equation, yielding the observed rate as 0.12 ± 0.03min^{-1} (half-life = 6 min). At least 3–4 kinetic traces were collected for each experimental condition, and they were averaged. The resultant kinetic traces were analyzed using an exponential rate equation, and the error in the measurement represents the standard error of the parameter derived from non-linear regression analysis using the Origin software package (OriginLab).

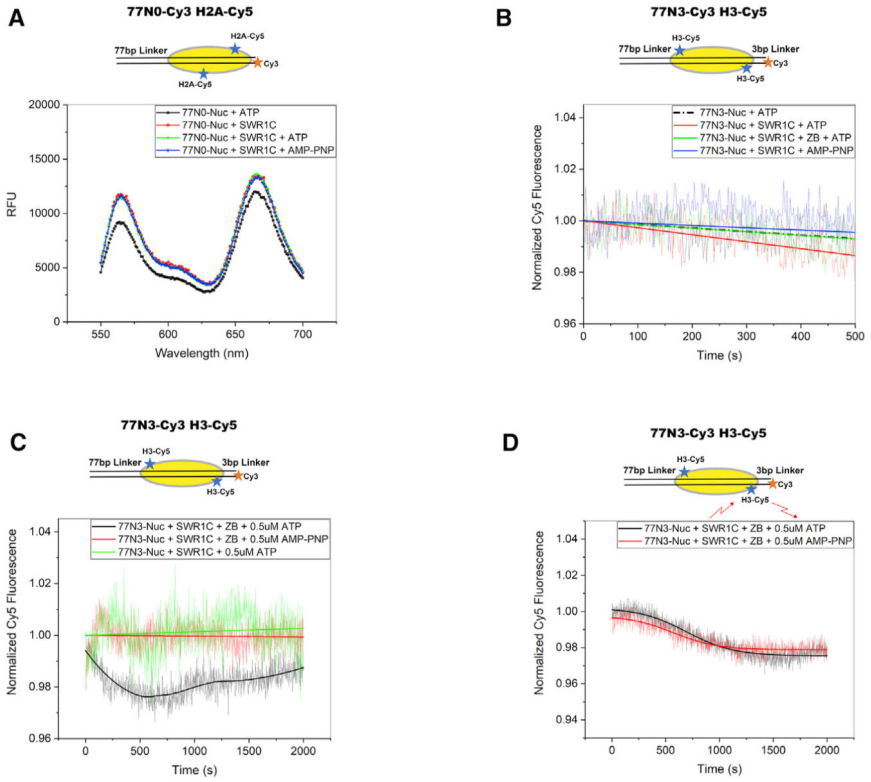

Figure 4. SWR1C Catalyzes ATP-Dependent Unwrapping of Nucleosomal DNA during Dimer Exchange

(A) The emission spectra under Cy3 excitation at 530 nm of 77N0-Cy3 H2A-Cy5 nucleosomes incubated with ATP (black), SWR1C (red), SWR1C and ATP (green), or SWR1C and AMP-PNP (blue).

(B) Normalized Cy5 FRET trace of 77N3-Cy3 H3-Cy5 nucleosomes incubated under saturating nucleotide concentrations with ATP (black); SWR1C and ATP (red); SWR1C and AMP-PNP (blue); or SWR1C, H2A.Z-H2B dimers, and ATP (green).

(C) Normalized Cy5 FRET trace of 77N3-Cy3 H3-Cy5 nucleosomes bound to SWR1C under low nucleotide concentrations with H2A.Z-H2B dimers and ATP (black), dimers and AMP-PNP (red), or no dimers and ATP (green).

(D) Normalized Cy5 signal under direct excitation at 650 nm showing no ATP-dependent change in the Cy5 environment for 77N3-Cy3 H3-Cy5 nucleosomes during SWR1C dimer exchange with low ATP concentration (black) compared with AMP-PNP (red).

The emission spectra in (A) were taken after 35 min of incubation, except for the reaction with the nucleosome and SWR1C, which was adjusted for photobleaching using the spectra from the nucleosome and ATP reaction pre- and post-incubation. Spectra were collected in triplicates. FRET reaction time course traces were collected in at least duplicates, averaged, and fit to a linear regression or single-exponential decay model. The y-intercept of each fit was normalized to 1.

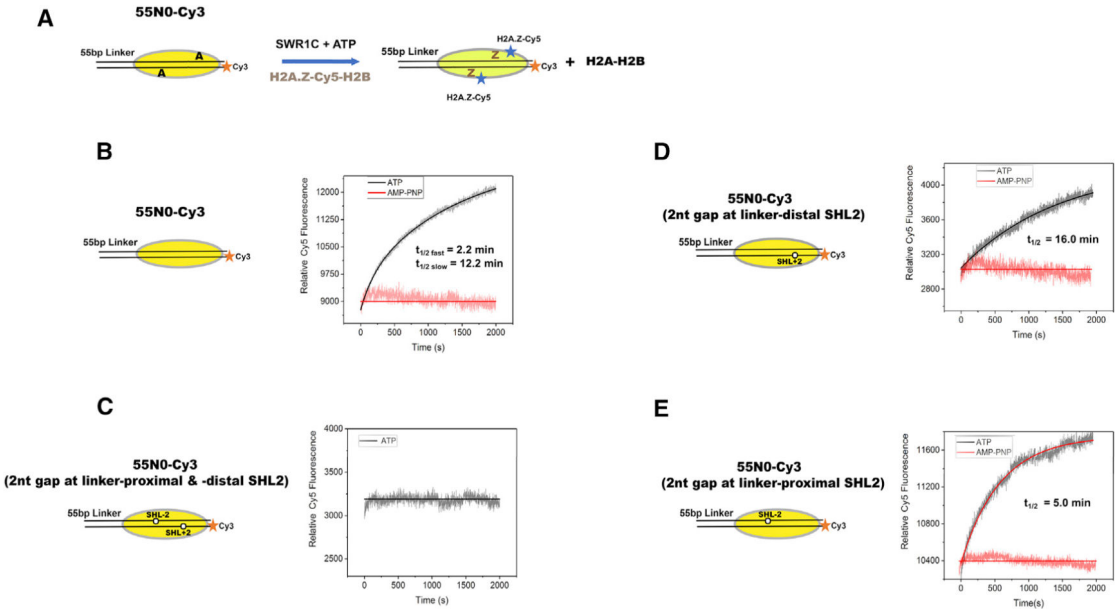

Figure 5. Transient Kinetics of ATP-Dependent Deposition of Two H2A.Z-H2B Dimers Is Asymmetric

(A) Experimental strategy for monitoring the rate of deposition of H2A.Z-H2B. The nucleosomal substrate contains only the Cy3-labeled DNA end, and Cy5 islocated on the free H2A.Z-H2B dimer (H2A.Z-C125-Cy5).

(B) Kinetic trace for the SWR1C-catalyzed deposition of the H2A.Z-H2B dimer to the intact H2A nucleosome. The biphasic trace was analyzed using a double-exponential rate equation, yielding the k_{obs} for the fast and slow phases as 0.31 ± 0.01 min^{-1} (half-life = 2.2 min) and 0.04 ± 0.01 min^{-1}(half-life = 16.6 min), respectively.

(C) Reactions as in (B), but the nucleosome contained 2-nt gaps at both SHL+2.0 and SHL −2.0.

(D) Same as in (B), but the reactions contained a nucleosome with a 2-nt gap at the linker-distal SHL+2.0. The monophasic trace was analyzed using a single-exponential rate equation, yielding the k_{obs} as 0.04 ± 0.01min^{-1}(half-life = 16 min).

(E) Reactions as in (B), but the nucleosome harbors a 2-nt gap at the linker-proximal SHL −2.0. The monophasic trace was analyzed using a single-exponential rate equation, yielding the observed rate as 0.14 ± 0.02 min^{-1}(half-life = 5 min).

At least 3–4 kinetic traces were collected for each experimental condition, and they were averaged. The resultant kinetic traces were analyzed using an exponential rate equation, and the error in the measurement represents the standard error of the parameter derived from non-linear regression analysis using the Origin software package (OriginLab).

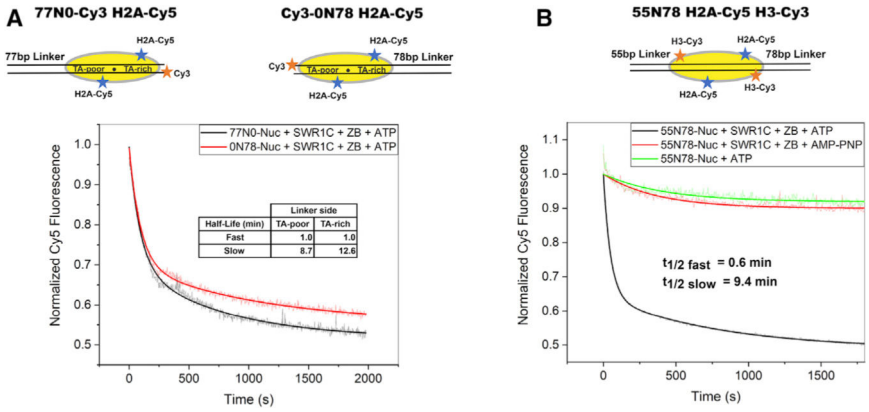

Figure 6. Nucleosome Determinants of Asymmetric Dimer Exchange

(A) Normalized Cy5 FRET signal comparing theSWR1C-dependent kinetics of H2A-Cy5 eviction from nucleosomes with the linker on the TA-poor (black) or TA-rich side (red) of the 601 nucleosome position sequence.

(B) Normalized Cy5 FRET signal showing biphasic kinetics of H2A-H2B dimer eviction from center-positioned 55N78 H3-Cy3 H2A-Cy5 nucleosomes by SWR1C and the H2A.Z-H2B dimer upon addition of ATP (black) compared with the negative controls of AMP-PNP (red) or nucleosome alone plus ATP (green). The half-lives of the fast and slow phase are 0.6 min and 9.4 min, respectively, slightly faster than the rates of dimer eviction on the asymmetric 55N0 nucleosome.

Traces were collected in triplicates, averaged, and fit to a double-exponential decay model. The y-intercept of each fit was normalized to 1.

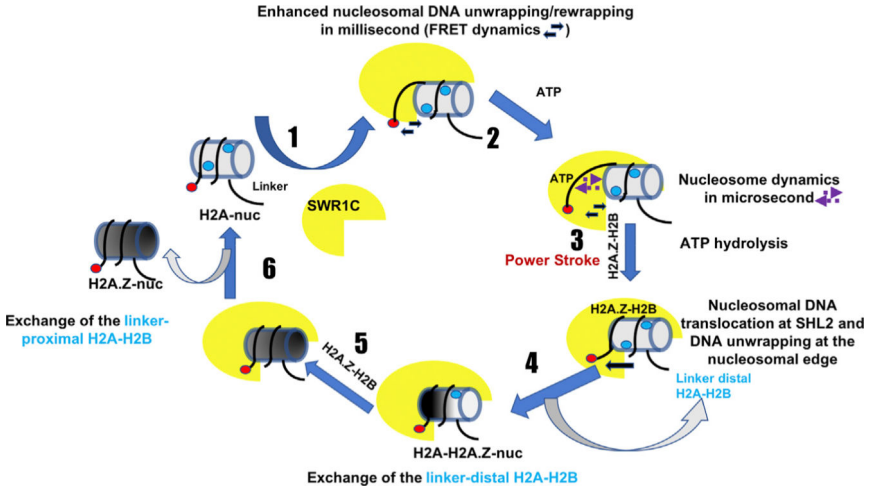

Figure 7. Kinetic Model of the SWR1C-Catalyzed Histone Dimer Exchange Reaction

(1) The engagement of SWR1C to the H2A-nucleosome enhances the unwrapping and/or rewrapping kinetics of the nucleosomal DNA on the millisecond timescale. (2) Binding of ATP to the SWR1C-engaged nucleosome further affects its dynamics on the microsecond timescale. (3) SWR1C and free H2A.Z-H2B dimers catalyze translocation of nucleosomal DNA, leading to unwrapping of DNA from the linker-distal nucleosome edge. We propose that this is the power stroke of the reaction. (4) Unwrapping of nucleosomal DNA leads to eviction and replacement of the distal H2A-H2B dimer. (5) SWR1C remains engaged with the H2A-H2A.Z heterotypic nucleosome and catalyzes the slower replacement of the linker-proximal H2A-H2B dimer, utilizing the H2A.Z-H2B-mediated second round of the power stroke.

KEY RESOURCES TABLE

REAGENT or RESOURCE	SOURCE	IDENTIFIER
Bacterial and Virus Strains		
Rosetta 2(DE3)pLysS	Novagen	71401–3
Rosetta 2	Novagen	71402–3
Chemicals, Peptides, and Recombinant Proteins		
Cy3 maleimide	Lumiprobe	41080
Cy5 maleimide	Lumiprobe	43080
Phusion High-Fidelity DNA Polymerase	New England Biolabs	M0530
Taq DNA Polymerase	New England Biolabs	M0273
USER Enzyme	New England Biolabs	M5505
S1 Nuclease	Thermo Fisher Scientific	18001016
3X FLAG Peptide	Millipore Sigma	F4799
Adenosine triphosphate disodium salt solution (ATP)	Sigma Aldrich	A6559
Adenosine 5′-(β,γ-imido)triphosphate lithium salt hydrate (AMPPNP)	Sigma Aldrich	10102547001
Phosphate Sensor	Thermo Fisher Scientific	PV4406
Phosphate Standard Solution	EMD Milipore	119898
Amicon Ultra 0.5ml centrifugal filter	Millipore Sigma	UFC5003
Critical Commercial Assays		
DNA Clean and Concentrator	Zymo Research	D4032
Experimental Models: Organisms/Strains		
Yeast Strain W1588–4C MATa *ade2–1 can1-100 his3–11,15 leu2–3,112 trp1–1 ura3–1 RAD5+ swr1::SWR1–3xFLAG-P-KanMX-P htz1*::natMX4)	Ranjan et al., 2013	N/A
Oligonucleotides		
55–601-TA poor side 5′-GGGAGCTCGGAACACTATCC-3′	This study	N/A
77–601-TA-poor side 5′-GTACCCGGGGATCCTCTAGAGT-3′	This study	N/A
0–601-TA-rich side 5′-CTGGAGAATCCCGGTGCC-3′	This study	N/A
Cy3–0-601-TA-rich 5′-Cy3-CTGGAGAATCCCGGTGCC-3′	This study	N/A
Cy3–3-601-TA-rich 5′Cy3-GCC TGGAGAATCC GGT-3′	This study	N/A
78–601-TA-rich 5′-GGATCCTAATGACCAAGGAAAGC-3′	This study	N/A
Cy3–0-601-TA-poor 5′-Cy3-ACAGGATGTATATATCTGACAC GTGC-3′	This study	N/A
Recombinant DNA		
pRET-yH2A-K120C	This Study	N/A
pRET-yH2AZ-K126C	This Study	N/A
pRET-yH2AZ	T. Richmond	N/A

REAGENT or RESOURCE	SOURCE	IDENTIFIER
pRET-yH2A	T. Richmond	N/A
pRET-yH3	T. Richmond	N/A
pRET-yH4	T. Richmond	N/A
pRET-xH4	T. Richmond	N/A
pRET-hH3.2-G33C	This Study	N/A
pGEM-601	This Study	N/A
Software and Algorithms		
ImageQuant	GE	http://www.gelifesciences.com/en/us/shop/protein-analysis/molecular-imaging-for-proteins/imaging-software/imagequant-tl-8--1-p--00110
OriginLab	OriginLab Corporation	https://www.originlab.com/
Burst Analyzer	Becker & Hickl GmBH	https://www.bec-ker-hickl.com/products/burst-analyzer/